Tarım Bilimleri Dergisi
Tar. Bil. Der.
Dergi web sayfası:
www.agri.ankara.edu.tr/dergi

Journal of Agricultural Sciences
Journal homepage:
www.agri.ankara.edu.tr/journal

TARIM BİLİMLERİ DERGİSİ — JOURNAL OF AGRICULTURAL SCIENCES 23 (2017) 147-155

Structural Analysis of Field Sprayer Booms

Caner Koc[a]

[a]*Ankara University, Faculty of Agriculture, Department of Agricultural Machinery and Technologies Engineering, 06110, Ankara, TURKEY*

ARTICLE INFO
Research Article
Corresponding Author: Caner Koc, E-mail: ckoc@ankara.edu.tr, Tel: +90 (312) 596 11 25
Received: 13 October 2015, Received in Revised Form: 28 December 2015, Accepted: 31 December 2015

ABSTRACT

In this paper, structural analysis of a 21 meters wide field sprayer boom, designed for precision agriculture applications, was conducted with finite element analysis. G-programming language, a data acquisition board and an inductive force transducer were used to measure the forces acting on the boom arms. An experimental setup, developed in a laboratory environment, was able to measure and record various forces in 5 miliseconds intervals. An ANSYS model was developed to analyze the forces recorded during laboratory experiments. Steel (SAE/AISI St 42) and aluminum (ISO AlMg2.5) materials for the sprayer boom structure were used in the analyses. Based on the analysis results, using aluminum for active boom suspension system for field sprayers produced more favorable structural results than steel.

Keywords: Transient analysis; Aluminum; Steel; G-Programming; Finite element analysis; ANSYS

Bir Tarla Pülverizatör Bumunun Yapısal Analizi

ESER BİLGİSİ
Araştırma Makalesi
Sorumlu Yazar: Caner Koc, E-posta: ckoc@ankara.edu.tr, Tel: +90 (312) 596 11 25
Geliş Tarihi: 13 Ekim 2015, Düzeltmelerin Gelişi: 28 Aralık 2015, Kabul: 31 Aralık 2015

ÖZET

Bu çalışmada, hassas tarımda kullanmak amacıyla tasarlanan 21 metre iş genişliğine sahip bir tarla pülverizatör bumunun sonlu elemanlar yöntemiyle yapısal analizleri gerçekleştirilmiştir. Bum kollarına gelen farklı kuvvet değerlerinin ölçümü için G-programı, bir adet veri algılama kartı ve indüktif bir kuvvet algılayıcısı kullanılmıştır. Laboratuvar ortamında geliştirilen deney düzeneği farklı kuvvet büyüklüklerini 5 milisaniye aralıklarla ölçerek kaydedebilecek şekilde hazırlanmıştır. Deneysel olarak elde edilen kuvvet verilerinin analizi için ANSYS ortamında bir model geliştirilmiştir. Analizlerde bum malzemesi olarak çelik (SAE/AISI St 42) ve alüminyum (ISO AlMg2.5) kullanılmıştır. Yapılan denemelerde elde edilen sonuçlara göre, aktif bum dengelemesi için alüminyum malzemenin yapısal olarak çeliğe göre daha iyi olduğu sonucuna varılmıştır.

Anahtar Kelimeler: Süreksiz analiz; Alüminyum; Çelik; Grafiksel programlama; Sonlu elemanlar; ANSYS

1. Introduction

Most of the machines used for agricultural operations are subjected to vibrations and oscillations due to irregular field conditions. Due to their large working widths, field sprayers are usually exposed to extreme vibrations and oscillations during field operations (Koc & Keskin 2011). Among the main reasons for non-uniform distributions of pesticides applied by field sprayers are the presence of oscillations and vibrations on the boom (Hedden 1961). The large working width and the vibration of field sprayer booms result in uneven clearance heights between the field sprayer boom and the field surface (Çilingir & Çelen 1995). To maintain a uniform pesticide distribution, an appropriate distance between the sprayer boom and the agricultural field surface must be maintained throughout the spraying operation (Pochi & Vannucci 2001; Jeon et al 2004).

In order to reduce fuel consumption and time during spraying, field sprayers with large working widths are used. However, as the width of the sprayer increases, the weight of the boom also increases. A 36 meters wide sprayer boom made of steel weighs approximately 1155 kilograms, whereas a similar boom with the same width made of aluminum weighs 770 kilograms. As in aviation industry, carbon fiber is becoming a more preferred material than steel or aluminum because of weight saving. A 36 meters wide sprayer boom made of carbon fiber weighs only 385 kilograms (Anonymous 2015a). However, the high cost of carbon fiber is the major factor limiting its use in field sprayers and other agricultural equipment.

Steel and aluminum are the most commonly used structural materials in agricultural machinery. Due to the higher resistance and relatively lower costs, steel materials are widely used in the sector. In the meantime, aluminum is also becoming a commonly used material in agricultural machinery because of its weight (Herrington & Latorre 1998; Lamb et al 2011).

When aluminum and steel are compared, aluminum is lighter, and has higher corrosion and temperature resistances than steel. However, aluminum is more expensive, has lower yield and tensile strengths, and lower fracture resistance than steel. The cost of steel, on the other hand, is inexpensive and has better welding and machining properties than aluminum (Kasten 2010).

Finite element analysis can be implemented to analyze the strength of a structure. Using finite element analysis, a structure's vibration response and factor of safety can be obtained very close to the real values in a short time (Moaveni 2007; Chu & Lei 2014) identified that the theoretical finite element analysis results of a boom structures were close to the results of experimental analysis.

In this study, the sprayer boom characteristics were determined with mechanical analysis. A model of the boom was then manufactured based on the results of mechanical analysis. The critical points of failure of the boom system were identified by using an electro-hydraulic simulation in laboratory conditions. The critical values were measured with sensors and a data acquisition system. A computer program was developed in Labview G-programming language for this research. Finite element analysis was carried out in ANSYS software based on the data collected with laboratory experiments. The model then was used for testing different materials for the sprayer boom structure. Two boom materials, steel SAE/AISI St 42, and aluminum ISO AlMg2.5 were tested with the developed model. Finally, the outputs of the model were compared with the results obtained from laboratory experiments.

2. Material and Methods

2.1. Materials

2.1.1. Field sprayer boom for laboratory experiments

A prototype field sprayer boom was manufactured for this research. The working width of the field sprayer was 21 meters with three major sections. Left and right sides of the boom were 9 meters long and the center was 3 meters wide. The boom was designed in a way that the left and right sections of the boom could move independently. The boom sections were manufactured from 3 meters long and 40x60x3 millimeters in cross-sectional dimensions of aluminum profile. The different motions of the boom sections were controlled using hydraulic cylinders. Two lifting cylinders were used to maintain the distance between the ground surface and each side of the boom, and one hydraulic cylinder was used to move the whole structure vertically (Figure 1).

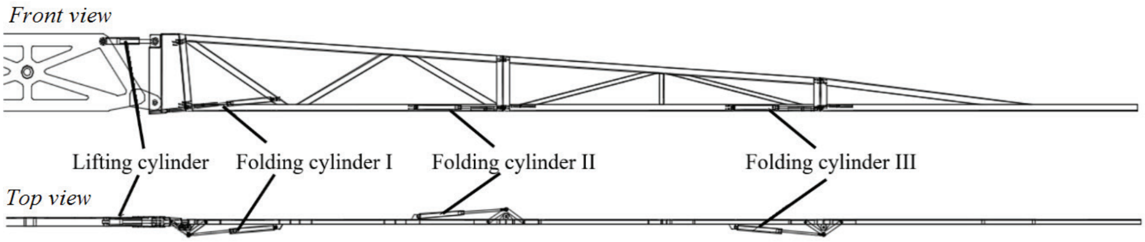

Figure 1- The sprayer boom structure used for the experiments

***Şekil** 1- Denemelerde kullanılan pülverizatör bumunun yapısı*

2.1.2. Load measurement set-up

An inductive force transducer and an NI 6009 data acquisition card were used for load measurements. A 30 millimeter diameter hydraulic cylinder was designed to mount and dismount the force transducer at the center of the field sprayer (Figure 2). The piston rod of the hydraulic cylinder was working as an inductive force measurement tool as well as a connecting part. The measurement set up was used to measure the upward and downward loads.

Figure 2- Load measurement set-up

Şekil 2- Kuvvet ölçüm düzeneği

2.1.3. Data acquisition

For data acquisition process, a graphical program was developed by using LABVIEW 8.2. The developed G-program facilitates the collection and recording of the inductive load data with the help of an NI 6009 data acquisition card to a personal computer. The inductive force measurements were displayed both in graphical and numeric indicators on the computer screen.

2.2. Method

2.2.1. ANSYS finite element formulation

2.2.1.1. Static analysis

The static mathematical formulas in the ANSYS program which are valid for all degrees of freedom are given in Equation 1 and 2. The effects of inertia and damping effects were neglected except for static acceleration fields (Anonymous 2015b).

$$[K]\{u\} = \{F\} \tag{1}$$

$$[K]\{u\} = \{F^a\} + \{F^r\} \tag{2}$$

$$[K] = Total\ stiffness\ matrix = \sum_{m=1}^{N} [K_e]$$

Where; $\{u\}$, nodal displacement vector; N, number of elements; $[K_e]$, elements stiffness matrix; $\{F^r\}$, reaction load vector; $\{F^a\}$, total applied vector.

Total applied vector defined in Equation 3.

$$\{F^a\} = \{F^{nd}\} + \{F^{ac}\} + \sum_{m=1}^{N}(\{F_e^{th}\} + \{F_e^{pr}\}) \quad (3)$$

Where; $\{F^{nd}\}$, applied nodal load vector; $\{F^{ac}\}$ = - $[M]\{a_c\}$, acceleration load vector; $[M]$, total mass matrix; $\{a_c\}$, total acceleration vector; $\{F_e^{th}\}$, element thermal load vector; $\{F_e^{pr}\}$, element pressure load vector.

The nodal displacements for one member of the boom structure are obtained as shown in Figure 3.

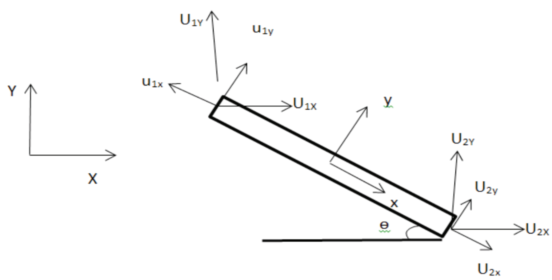

Figure 3- Static mode displacements of one member of the boom

Şekil 3- Bum üzerindeki bir noktanın static mod yer değişimi

X-Y axis in Figure 4 indicates the global coordinate system, and *x-y* indicates the local coordinate system. The angle between the element member and the horizontal plane is shown with ө. The displacements at two nodes (node 1 and node 2) are shown in both coordinate systems. The global displacements (U) are related to the local displacements (u) determined from the Equation 4-8.

$$U_{1X} = -u_{1x}\sin(\theta) + u_{1y}\cos(\theta) \quad (4)$$

$$U_{1Y} = u_{1x}\sin(\theta) + u_{1y}\cos(\theta) \quad (5)$$

$$U_{2X} = u_{2x}\cos(\theta) + u_{2y}\sin(\theta) \quad (6)$$

$$U_{2Y} = -u_{2x}\cos(\theta) + u_{2y}\sin(\theta) \quad (7)$$

$$\{U\} = [T]\{u\} \quad (8)$$

Where; T, transformation matrix.

Transformation matrix is shown in Equation 9.

$$[U] = \begin{bmatrix} U_{1x} \\ U_{1y} \\ U_{2x} \\ U_{2y} \end{bmatrix},\ [T] = \begin{bmatrix} -\sin(\theta) & \cos(\theta) & 0 & 0 \\ \sin(\theta) & \cos(\theta) & 0 & 0 \\ 0 & 0 & \cos(\theta) & \sin(\theta) \\ 0 & 0 & -\cos(\theta) & \sin(\theta) \end{bmatrix},\ [u] = \begin{bmatrix} u_{1x} \\ u_{1y} \\ u_{2x} \\ u_{2y} \end{bmatrix} \quad (9)$$

The reaction force values were calculated using the Equation 10-12.

$$\{F\} = [T]\{f\} \quad (10)$$

The relations between the node forces and the displacements are similar to a linear spring.

$$F = KX \quad (11)$$

$$\{f\} = K\{u\} \quad (12)$$

K is related to the property of the material given by Equation 13.

$$K = A \cdot E \cdot L^{-1} \quad (13)$$

Where; A, cross sectional area; L, length and E, modulus of elasticity of the element member.

After substituting for $\{f\}$ and $\{u\}$ in terms of $\{F\}$ and $\{U\}$ and multiplying both sides with $[T]$ F can be written as Equation 14.

$$[F] = K[T]^{-1}[U][T] \quad (14)$$

The matrix of nodal forces were determined by substituting the values of the $\{F\}$, $[T]^{-1}$, $[T]$, and $\{U\}$ matrices and multiplying (Equation 15).

$$\begin{bmatrix} F_{1x} \\ F_{1y} \\ F_{2x} \\ F_{2y} \end{bmatrix} = k \cdot \begin{bmatrix} -\sin(\theta) & \cos(\theta) & 0 & 0 \\ \sin(\theta) & \cos(\theta) & 0 & 0 \\ 0 & 0 & \cos(\theta) & \sin(\theta) \\ 0 & 0 & -\cos(\theta) & \sin(\theta) \end{bmatrix} \begin{bmatrix} -\sin(\theta) & \cos(\theta) & 0 & 0 \\ \sin(\theta) & \cos(\theta) & 0 & 0 \\ 0 & 0 & \cos(\theta) & -\cos(\theta) \\ 0 & 0 & \sin(\theta) & \sin(\theta) \end{bmatrix} \begin{bmatrix} u_{1x} \\ u_{1y} \\ u_{2x} \\ u_{2y} \end{bmatrix} \quad (15)$$

The same principle was applied for all of the members of the structure and finally the element stiffness matrices were obtained. The equation was then solved by applying boundary conditions and loads, which produced the displacement stresses.

2.2.1.2. Transient analysis

A transient dynamic analysis was used to determine the response of the boom structure under time-depended loading with inertia and damping effects. The transient analysis solution method (ANTYPE, TRANS) was dependent on the degrees of freedom. The most widely used finite element discrete equation of motion for dynamic structures were the virtual work method given in Equation 16.

$$[M]\{\ddot{u}(t)\}+[C]\{\dot{u}(t)\}+\{F^{i}(t)\}=\{F^{a}(t)\} \qquad (16)$$

Where; $[M]$, structural mass matrix; $[C]$ $\{\ddot{u}(t)\}$, structural damping matrix; $\{\ddot{u}(t)\}$, nodal acceleration vector; $\{\dot{u}(t)\}$, nodal velocity vector; $\{u(t)\}$, nodal displacement vector; $\{F^{i}(t)\}$, internal load vector; $\{F^{a}(t)\}$, applied load vector.

In linear structural dynamics systems, the internal load is linearly proportional to the displacement while the structural stiffness matrix remains constant. Therefore, Equation 16 was rewritten as Equation 17.

$$[M]\{\ddot{u}(t)\}+[C]\{\dot{u}(t)\}+[K]\{u(t)=\{F^{a}(t)\} \qquad (17)$$

Where; $[K]\{u(t)\}$, structural stiffness matrix.

In addition to the above given direct time integration methods, other methods of solving transient problems were also included in ANSYS; such as the new method, generalized -α method, the Hilber Hughes-Taylor (HHT) method, and the Newmark family of time integration algorithms.

2.2.2. ANSYS graphical modeling

Modeling of the system in ANSYS was started by developing the mesh structure and assuming the boundary conditions. The boundary conditions used in the model are shown in Table 1.

2.2.3. Laboratory experiments

The loads on the boom joints were measured by using the inductive transducer. This transducer is attached at the center of 30 millimeters diameter piston with a specially constructed screw profile. The other end of the transducer was then attached to the boom elements. The measurements of the load were recorded with the NI 6009 data acquisition card on the computer. For the upward and downward movements of the boom structure, especially designed hydraulic cylinders were used. The cylinders were driven by the hydraulic output of the tractor. During the experiments, the tractor hydraulic system output pressure of 120 bars was used. To measure the static loads on the boom structure and the joints, calibrations were made by hanging known weights on three points of the 9 meters long boom structure. Following the calibration, static load data were collected. The data were then used as input for the ANSYS modeling.

Based on the inductive load data from the known masses a calibration equation was developed. The derived equation was then used in the Labview program. The derived equation with the coefficient of determination (R^2) value of 0.99 is shown in Equation 18.

$$y = 11.304x + 0.8952 \qquad (18)$$

Where; y, force (N) measured with the load sensor and x, known mass (kg).

Table 1- Boundary conditions used for the ANSYS model

Çizelge 1- Kullanılan ANSYS modeli üzerindeki sınır koşulları

Sizing		*Statistics*	
Use advanced size function	On: Curvature	Nodes	819202
Relevance center	Fine	Elements	518338
Curvature normal angle	12.0°	Aspect ratio	
Min size	5.0 mm	Min	1.16
Max face size	10.0 mm	Max	44.5
Max size	20.0 mm	Average	1.88
Growth rate	1.20		
Minimum edge length	1.7857e-002 mm		

Based on the calibration equation in the computer program, the unknown force values were obtained in 5 milliseconds intervals.

3. Results and Discussion

3.1. Results

The results of the ANSYS structural analyses are given in Table 2 and Figures 4. Based on the loads on the boom structure, static and transient analyses were performed in ANSYS environment. Total deformation, equivalent stress and safety factor values on aluminum and steel boom structures were obtained from the analyses. Based on the static analysis that the total deformation on the aluminum structure was 27 mm, total stress was 189 MPa and the minimum critical safety factor was 0.45. On the other hand, the total deformation on the steel structure was 19 mm, total stress was 399.67 MPa and the minimum safety factor was 0.21.

In addition to the structural analysis, a transient analysis was also conducted. The critical values of the transient analysis are tabulated in Table 3. The transient analyses showed that the total deformation, equivalent stress and safety factor values for both aluminum and steel were obtained at 0.0025 s, 0.5 s and 1.0 s, respectively. For both materials, the critical safety factor values were obtained at 1.0 s. Transient analyses also showed that for aluminum structure, the total deformation was 29.33 mm, total stress was 220 MPa and the critical minimum safety factor was 0.39. For steel structure, these values were as 31.14 mm, 664 MPa and 0.12, respectively.

3.2. Discussion

According to the structural and transient analyses, aluminum boom material produced greater factor of safety than steel, which is the better material of the two for field sprayer boom construction. This is due to the fact that aluminium is lighter in weight because of the internal molecular and mechanical properties (Kuziak et al 2008).

The critical points of failure observed during laboratory experiments overlapped with the critical

Table 2- Static analysis results

Çizelge 2- Statik analiz sonuçları

Parameters	*Steel (SAE/AISI St 42)*		*Aluminum (ISO AlMg2.5)*	
	Min	*Max*	*Min*	*Max*
Total deformation (mm)	0	19	0	27
Equivalent stress (MPa)	0.017	399.67	0.0031	189
Safety factor	0.21	15	0.45	15

Table 3- Transient analysis results

Çizelge 3- Zamana bağlı analiz sonuçları

Parameter	*Steel (SAE/AISI St 42)*						*Aluminum (ISO AlMg2.5)*					
	0.0025 s		*0.5 s*		*1 s*		*0.0025 s*		*0.5 s*		*1 s*	
	Min	*Max*	*Min*	*Max*	*Min*	*Max*	*Min*	*Max*	*Min*	*Max*	*Min*	*Max*
Total deformation (mm)	0	1.69	0	14.64	0	31.14	0	1.70	0	13.59	0	29.4
Equivalent stress (MPa)	0	136	0	359.97	0	664	2.4	42.28	0	112.56	0	220
Safety factor	0.6	15	0.234	15	0.12	15	2.03	15	0.76	15	0.39	15

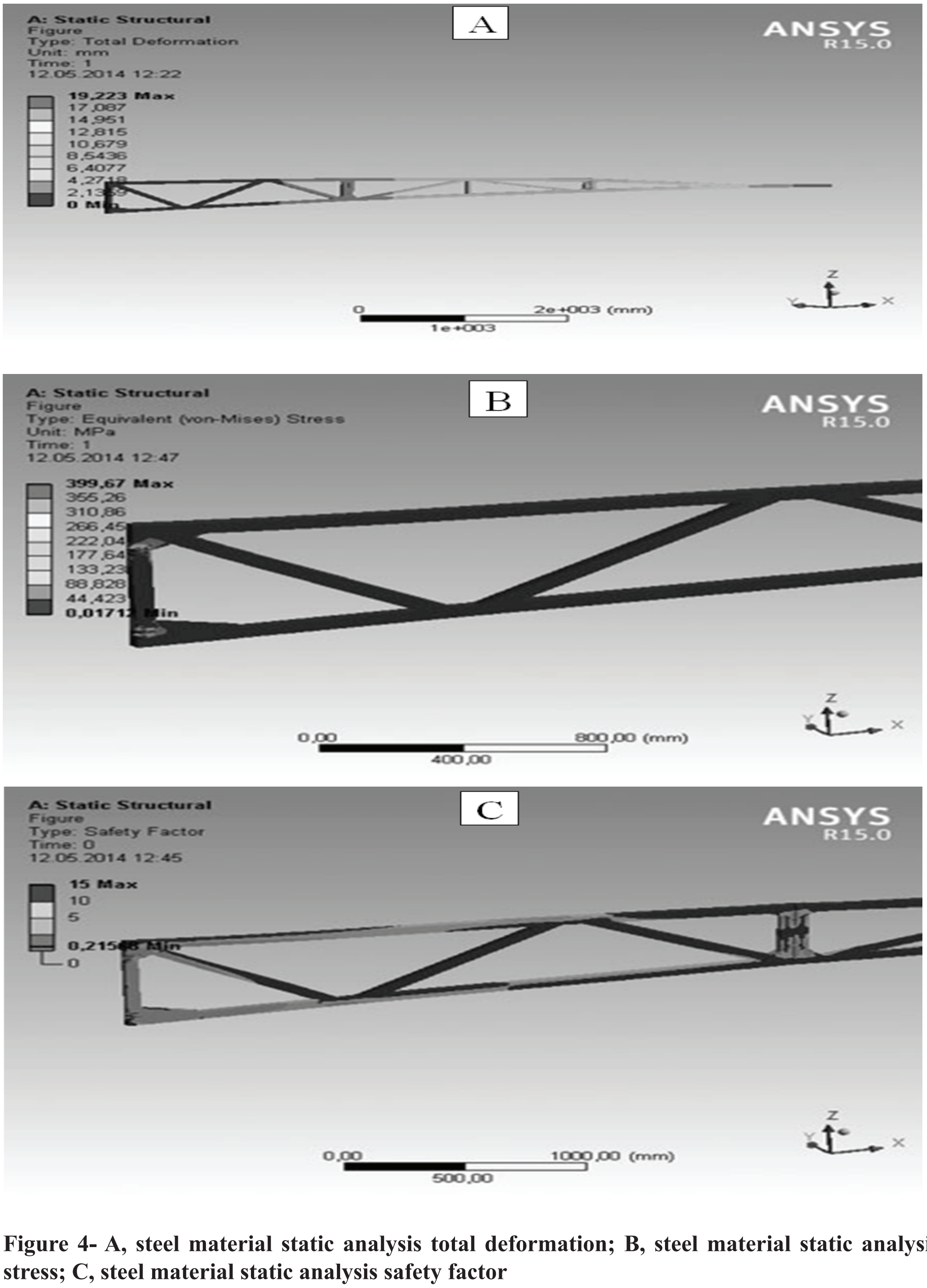

Figure 4- A, steel material static analysis total deformation; B, steel material static analysis equivalent stress; C, steel material static analysis safety factor

Şekil 4- A, çelik malzeme static analiz güvenlik faktörü; B, çelik malzeme statik analiz toplam yer değişimi; C, çelik malzeme static analiz eş değer gerilme points identified by the ANSYS analysis. The failure points of the boom structure observed during experimental activities as shown in Figure 5. The point of failure was also identified during designing the boom.

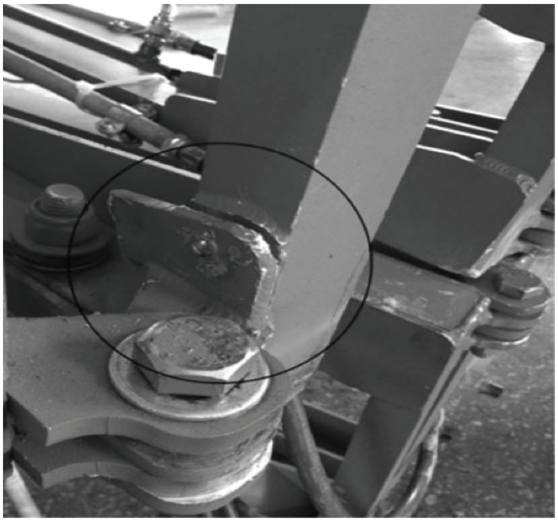

Figure 5- Sprayer boom failure point during experiments

Şekil 5- Denemeler sırasında pülverizatör bumu üzerinde görülen kopma

The same points of failures were also identified by the modeling and analysis using ANSYS prior to experimental failures for both steel and aluminum boom materials. Thus, instead of materials (aluminum or steel), boom design should be renewed. For this purpose, dismountable joint aluminum alloy material can be used.

Due to the higher strength of aluminum, one can say that aluminum is better than steel for boom construction. Moreover, the lighter weight of aluminum has an advantage to save fuel consumption of tractors due to the lower loads on the tractor carrying the field sprayer.

Zhou et al (2011) reported that vehicles made of aluminum were lighter than the ones made of steel hence improving the fuel efficiency. One of the problems for field sprayer booms is the collision with the ground and the breakdown of boom structures during field operations. Materials with higher spring properties are desired to reduce the breakdown due to collisions with the ground. The solution used by the automobile industry to solve this problem, which is using aluminum and Advanced High Strength Steels (AHSS) can be adapted for boom manufacturing too. The workability of aluminum is also better than that of steel. Nowadays, lighter weight with high strength like the AHSS can be used as an alternative to aluminum for boom manufacturing (Anonymous 2015c). Although the price of aluminum is expensive than that of steel by at least 30%, aluminum has many other advantages than steel that it is preferred as a boom material.

4. Conclusions

According to this research, it is concluded that field sprayer booms constructed from aluminum are better than steel constructed booms. During the experiments, it was observed that the critical point of failure of the booms is at the universal joint connection of the boom wings to each other. The critical point of failure of the booms found during the experimental analysis was the same point found by using the structural and transient ANSYS analysis of the system. From this research, it can be concluded that maximum care must be given to the critical point of failures mentioned above during the design of field sprayer booms.

References

Anonymous (2015a). New aluminum boom options. http://www.farmindustrynews.com (Access date: April 12, 2015)

Anonymous (2015b). ANSYS. http://www.ansys.com/Products/Structures (Access date: June 12, 2015)

Anonymous (2015c). Steel beats aluminum. http://www.autosteel.org (Access date: May 12, 2015)

Chu Z Y & Lei Y A (2014). Design theory and dynamic analysis of a deployable boom. *Mechanism and Machine Theory* **71**: 126-141

Çilingir İ & Çelen İ H (1995). Tarla pülverizatörlerinde bum stabilitesi. *Tekirdağ Ziraat Fakültesi Dergisi* **4**(1-2): 157-167

Hedden O K (1961). Spray drop sizes and size distribution in pesticide sprays. *Transactions of the ASAE* **4**(2): 158-159

Herrington P D & Latorre R G (1998). Development of an aluminum hull panel for high-speed craft. *Marine Structures* **11**: 47-71

Jeon H Y, Womac A R & Gunn J (2004). Sprayer boom instrumentation for field use. *American Society of Agricultural Engineers* **47**(3): 659-666

Kasten M (2010). Strength of aluminum vs. strength of steel. http://www.kastenmar ine.com/alum VS steel. htm (Erişim tarihi: 09.10.2016)

Koc C & Keskin R (2011). Tarla pülverizatörleri için pic kontrollü aktif bir bum dengeleme sisteminin geliştirilmesi. *Tarım Bilimleri Dergisi-Journal of Agricultural Sciences* **17**: 1-13

Kuziak R, Kawalla R & Waengler S (2008). Advanced high strength steels for automotive industry. *Archives of Civil and Mechanical Engineering* **3**(2): 103-117

Lamb T, Beavers N, Ingram T & Schmieman A (2011). The benefits and cost impact of aluminum naval ship structure. *Journal of Ship Production and Design* **27**: 35-49

Moaveni S (2007). Finite Element Analysis Theory and Application with ANSYS. Third Edition, *Pearson Education International*: New Jersey ISBN-10: 0131890808

Pochi D & Vannucci D (2001). Labaratory evaluation of linear and angular potentiometers for measuring spray boom movements. *Journal of Agricultural Engineering Research* **80**(2): 153-161

Zhou Y J, Lan F & Chen J (2011). Crashworthiness research on S-shaped front rails made of steel-aluminum hybrid materials. *Thin-Walled Structures* **49**: 291-297